Spectrochimica Acta Part A: Molecular and Biomolecular Spectroscopy 127 (2014) 490–497

Contents lists available at ScienceDirect

Spectrochimica Acta Part A: Molecular and Biomolecular Spectroscopy

journal homepage: www.elsevier.com/locate/saa

Comparative experimental and theoretical studies of N-(4-Methylbenzylidene)-N′-(2-carboxyphenyl) hydrazine novel Schiff base

Tuncay Tunç [a,*], Habibe Tezcan [b], Semran Sağlam [c], Nefise Dilek [d]

[a] *Aksaray University, Education Faculty, Department of Science Education, Aksaray, Turkey*
[b] *Gazi University, Education Faculty, Department of Chemistry Education, Ankara, Turkey*
[c] *Gazi University, Faculty of Sciences, Physics Department, 06500 Ankara, Turkey*
[d] *Aksaray University, Arts and Sciences Faculty, Department of Physics, Aksaray, Turkey*

HIGHLIGHTS

- N-(4-Methylbenzylidene)-N′-(2-carboxyphenyl) hydrazine.
- Elemental analyses, UV–Vis and IR spectroscopy and single crystal X-ray determination.
- The density functional theory (DFT) B3LYP method using the 6-311++G(d,p) basis set.
- The calculated geometry parameters, IR and UV–Vis results were compared with experimental results.

GRAPHICAL ABSTRACT

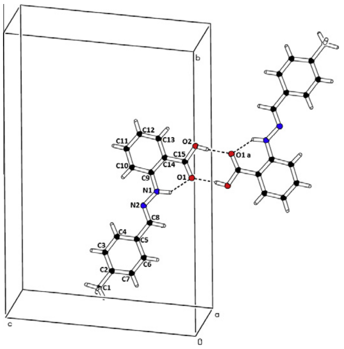

ARTICLE INFO

Article history:
Received 30 December 2013
Received in revised form 12 February 2014
Accepted 16 February 2014
Available online 4 March 2014

Keywords:
Hydrazone
Condensation reaction
Crystal structure
DFT

ABSTRACT

In this work, N-(4-Methylbenzylidene)-N′-(2-carboxyphenyl) hydrazine, $C_{15}H_{14}N_2O_2$, Schiff base molecule has been synthesized and characterized by elemental analyses, UV–Vis and IR spectroscopy and single crystal X-ray determination. The molecule of the title compound adopt an E configuration about the azomethine C═N double bond. The benzene and phenyl rings are planar and the dihedral angle between the planes is 7.2(2)°. The crystal structure is stabilized by intermolecular O—H···O and intramoleculer N—H···O hydrogen bonding interactions. X-ray diffraction analyses show that, N-(4-Methylbenzylidene)-N′-(2-carboxyphenyl) hydrazine Schiff base molecule crystallizes in the monoclinic system, $P2_1/c$ space group, $a = 4.392(5)$ Å, $b = 22.340(5)$ Å, $c = 13.528(5)$ Å, $\beta = 92.882(5)°$, $V = 1325.7(16)$ Å^3, $Z = 4$. The conformational analysis of N-(4-Methylbenzylidene)-N′-(2-carboxyphenyl) hydrazine was performed by the density functional theory (DFT) B3LYP method using the 6-311++G(d,p) basis set. Also, theoretical values of FTIR and UV–Vis were performed by the same method. The calculated geometry parameters, IR and UV–Vis results were compared with experimental results.

Introduction

Hydrazones, Schiff bases, are formed by the condensation of hydrazines with aldehydes or ketones. These are typically crystalline compounds with sharp melting points. Therefore, these

---

* Corresponding author. Tel.: +90 382 288 2228; fax: +90 382 288 22 26.
E-mail address: tctunc@gmail.com (T. Tunç).

http://dx.doi.org/10.1016/j.saa.2014.02.104
1386-1425/© 2014 Elsevier B.V. All rights reserved.

compounds can be used to identify the aldehydes and ketones from which the hydrazones have been formed. Hydrazones are more efficient than oximes in this reaction, because their greater molecular weight causes a lower solubility in most solvents. Therefore, they can be easily isolated and recrystallized [1]. Hydrazones are also useful for the synthesis of metal complexes as they easily form stable complexes with most transition metal ions. Therefore, hydrazones and their metal complexes have gained a special attraction and growing interest in chemistry and biology, analytical chemistry. Also, hydrazones possessing an azomethine —NHN═CH— proton constitute an important class of compounds for new drug development [2]. Also, hydrazones have been intensively investigated mostly for pharmacological applications due to their potential application as anticancer, antiviral, antibacterial, and antifungal agents [3–9]. Moreover, aromatic hydrazone molecules dispersed in a binder polymer are used as the main constituent of electro photographic photoreceptors of laser printers due to their excellent hole-transporting properties and relatively simple synthesis [10].

In this study, a new Schiff-base complex N-(4-Methylbenzylidene)-N′-(2-carboxyphenyl) hydrazine (MCH) has been synthesized and its structure was determined using the X-ray diffraction method. This compound is also characterized by elemental analysis, FT-IR, ^{1}H NMR and UV–Vis spectroscopy techniques. In the conformational analysis, the minimum energy conformational geometries were performed with the help of potential energies barrier by B3LYP/6-31 G basis set. In addition, we performed the structural and vibrational properties of the MCH molecule by means of DFT calculations using the B3LYP functional with 6-311++G** basis set. The complete assignment of the bands observed in the vibrational spectra were performed taking into account the natural internal coordinates for the more stable structures by using the harmonic force field with the Scaled Quantum Mechanics Force Field (SQMFF) methodology. The experimental and theoretical results were compared with each other.

Computational detail

All calculations were performed at density functional theory [11,12] using Gaussian 09 program [13], invoking gradient geometry optimization [14]. Geometry optimization, Harmonic vibrational spectra, NMR and UV–Vis spectra were performed using the Becke's three parameter hybrid functional, a combination that gives rise to the well known B3LYP method with 6-311++G(d,p) basis set [15–18]. Later, based on the SQMFF procedure [19], the harmonic force fields for the more stable conformer were evaluated at the same theory level. The theoretical vibrational spectra of the title compound were interpreted by means of TEDs using the SQM program [20]. Only the total energy distribution (TED) components ≥10% was considered to perform the final assignment.

The aim of the conformational analysis of the MCH molecule is to provide a model for the molecular structure. The energy barrier of the rotation around the $C_1—C_2$, $N_2—C_8$, $C_8—C_5$, $N_1—N_2$, $C_9—N_1$ and $C_{14}—C_{15}$ bond were calculated for by B3LYP/6-31G(d,p) basis set. All dihedral angles were varied from 0° to 360° by steps of 10°. All potential energy barriers are given in Fig. S1. The most stable geometry is shown in Fig. S1. The optimized geometric parameters (bond lengths, bond angles and dihedral angles) of the ground state are given in Table S1.

Then, the optimized molecular structure, vibrational normal modes, nuclear magnetic resonance spectra and UV–Vis spectra were calculated for ground state in the B3LYP with 6-311++G(d,p) basis sets.

Experimental

General procedures and materials

2-Hydrazinobenzoic acid and 4-methylbenzaldehyde were purchased from Aldrich and used without further purification. Ethanol and dioxan were purchased from Carlo Erba. All other chemical substances used were reagent-grade commercial products. The IR spectra were recorded on a THERMO NICOLAT 6700 ATR spectrophotometer by using KBr disk in the range 4000–400 cm^{-1}. The electronic spectra in the 200–780 nm range were obtained on a Shimadzu UV-1240 spectrophotometer using methanol as the solvent. Elemental analyses for (C, H, N) were performed using a LECO CHNS 932 elemental analyzer. ^{1}H NMR spectra were performed on a Bruker AVANCE DPX-300 MHz and Mass spectra were recorded using an Agilent 1100 MSD mass spectrometer.

Synthesis of compound MCH

The title compound, MCH, was prepared as shown in Scheme 1. For synthesis of the MCH, a solution of 4-methylbenzaldehyde (**1**) (2.403 g, 0.02 mol) in hot methanol (50 ml) was added dropwise to a solution of 2-hydrazinobenzoic acid (**2**) (3.77 g, 0.02 mol) in hot methanol–dioxane mixture (100:20 ml) and a little 5%HCl with constant stirring. Since condensation reaction was carried out in acidic conditions, synthesis was made at about pH 4–5 [21]. The procedure was completed in approximately 30 min. The resulting pale yellow Schiff base (**3**) was left on the bench for 3 days and then was filtered. The precipitate formed was filtered and the residue was dissolved in hot methanol under the reflux for 3 h. and kept in cupboard for 2 days for recrystallization and then was filtered. Also, a structure unsubstituted, N-benzlidene-N′-phenyl hydrazine (BPH) was synthesized in the same way for clarification of substituent effects of MCH. Experimental data of MCH Schiff base is given in Table S2.

X-ray diffraction study

The crystal and instrumental parameters used in the unit-cell determination and data collection are summarized in Table 1. Diffraction measurements were made at room temperature on a four-circle Rigaku R-AXIS RAPID-S diffractometer (equipped with a two-dimensional (2D) area IP detector). The graphite-monochromatized Mo Kα radiation ($\lambda = 0.71073$ Å) and oscillation scans technique with $\Delta\omega = 5°$ for one image were used for data collection. The lattice parameters were determined by the least-squares methods on the basis of all reflections with $F^2 > 2\sigma(F^2)$. Integration of the intensities, correction for Lorentz, and polarization effects, and cell refinement were performed using Crystal – Clear (Rigaku/MSC, Inc., The Woodlands, TX) software [22]. The structures were solved by direct methods using SHELXS-97 [23] and refined by a full matrix least-squares procedure using the program SHELXL-97 [24]. All non-hydrogen atoms were refined with anisotropic displacement parameters and hydrogen atoms were included in their idealized positions and refined isotropically. An ORTEP [25] drawing of the molecule with 50% probability displacement thermal ellipsoids and atom-labeling scheme are shown in Fig. 1.

Results and discussion

Vibrational spectra

Table 2 lists the results of three DFT calculations of the normal modes of vibration that were performed using the Gaussian 09 [13]

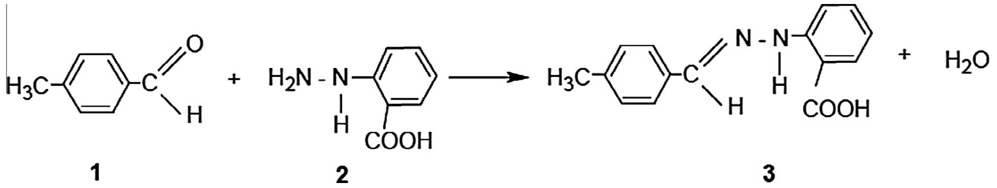

Scheme 1. Synthetic pathway for the synthesis of MCH Schiff-base.

Table 1
Crystal data and structure refinement details for MCH.

CCDC no.	913886
Chemical formula	$C_{15}H_{14}N_2O_2$
Formula weight (g/mol)	254.28
Space group	$P2_1/c$
Z	4
Crystal color/shape	Yellow/prism
a, b, c	4.3919(3), 22.3401(18), 13.528(2) Å
β (Å)	92.882(8)°
V (Å^3)	1325.7(2)
D_x (g/cm^3)	1.274
Radiation, λ	Mo Kα, 0.71073 Å
μ (mm^{-1})	0.086
T	293(2) K
$F(000)$	536
$T_{\min}$, $T_{\max}$	0.980,0.991
Scanning mode	$\omega/2\theta$
Scan range	$-6 \leqslant h \leqslant 5$, $-31 \leqslant k \leqslant 31$, $-19 \leqslant l \leqslant 19$
θ_{min}, θ_{max}	2.37–30.7
Reflections collected/unique/R_{int}	25296/4074/0.2621
Refinement method	Full-matrix least-squares on F^2
Number of reflections with $I > 2\sigma(I)$	2039
Number of refined parameters	183
Number of refined restraints	0
S	0.906
Final R indices [$I > 2\sigma(I)$]	$R_1 = 0.0672$, $wR_2 = 0.136$
R indices (all data)	$R_1 = 0.2605$, $wR_2 = 0.2147$
$\Delta\rho_{max}$, $\Delta\rho_{min}$ (e Å^{-3})	0.129, −0.14

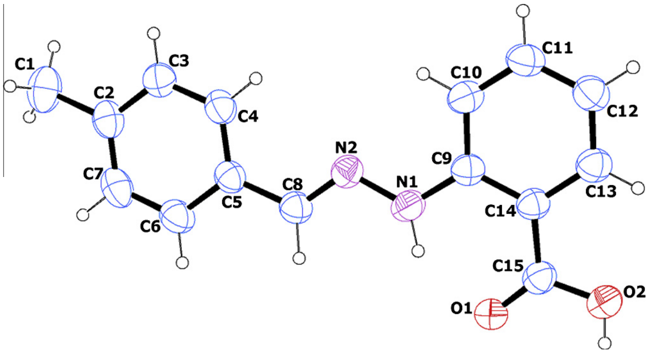

Fig. 1. ORTEP drawing of the title compound, represented with displacement ellipsoids are drawn at 50% probability level and showing the labeling scheme.

program package. These results were obtained using the B3LYP functional with the 6-311++G(d,p) basis set. The MCH molecule has 33 atoms, which possess 93 normal modes of vibrations. MCH molecule belongs to C_1 symmetry. All vibrations are active in infrared spectra. The recorded FT-IR spectral data, calculated wave numbers and IR intensities are given in Table 2. The total energy distributions for all fundamental vibrations were calculated using scaled quantum mechanics (SQM) method at B3LYP/6-311++G(d,p) level.

The selected IR spectral data of MCH Schiff base are given in Table 1 and the spectrum is shown in Fig. 2. Phenyl rings with methyl and carboxyl substituent are attached on the MCH. Owing to this structure, the IR spectrum of Schiff base MCH is different from BPH [26]. In the IR bands of MCH, N—H and aromatic C—H bands were observed at 3289–2300 cm^{-1} low intensity and broad according to BPH. The band at 3289 cm^{-1} was assigned to the ν (N—H) stretching frequency. N—H band was theoretically found 3271 cm^{-1} by B3LYP level of theory. Aromatic CH stretching vibrations are predicted at 3082–3011 cm^{-1} region by DFT calculation (Mode nos: 91-84). Experimental CH stretching vibration was measured at 3013 cm^{-1} in the FT-IR spectra. CH3 stretching vibrations are lower than those of aromatic ring. The experimental and theoretical results are quite compatible with each other [27,28].

The carbonyl stretching frequency has been most extensively studied by infrared spectroscopy. The CO stretch of carboxylic acids are found in the region 1780–1700 cm^{-1} [29,30]. In this work, CO stretching vibration has a main contribution in the mode no. 79, with B3LYP/6-311++G(d,p) determined at 1671 cm^{-1} and the values are observed at 1651 cm^{-1} as a strong peak. Indeed, on inter–intra molecular bonding, the CO stretching vibration of carboxyl acid vibration is shifted slightly to lower wavenumbers.

Also, strong sharp bands were observed in the IR spectrum of Schiff base at 1439 cm^{-1} (mode nos: 70) and at 1602 cm^{-1} (mode nos: 78). According to the TED results, mode nodes 70 were predicted as CH in plane bending vibrations. This frequency is mixing mode with CC stretching vibration. As seen in Table 2, mode nos: 78 was determined as a C═N (44%) and C═C (29%). This frequency is assigned to the C═N stretching vibrations. These respective values were found at 1606 cm^{-1} and 1641 cm^{-1} theoretically. Furthermore, in the IR spectrum, an intensive band appeared at 1233 cm^{-1}, which is assigned to the in plane vibration of ring [31]. The vibration frequency value was found at 1228 cm^{-1} theoretically. The bending value was found at 1437 and 1367 cm^{-1} for CH_3 theoretically. All these vibration bands were observed in the expected regions [26,28,31–33]. Theoretically, C═NN bending and CC stretching in CNNC skeleton were observed at 893 cm^{-1} and were determined at 653 cm^{-1} as NH out-of-plane bending vibration.

In the IR spectra, three intensity bands appear at 1505, 1150–1000 and 742 cm^{-1}, which are assigned to vibration frequency v(phenyl ring stretching), v(phenyl ring bending) and v(phenyl ring out-of-plane), respectively. Theoretically, these values were found at 1547 cm^{-1} for v(phenyl ring stretching), 1105, 1132, 1161, 1228 and 1294 cm^{-1} for v(phenyl ring bending) and 967, 956, 943, 937, 913, 847, 802, 737 cm^{-1} for v(phenyl ring out-of-plane bending vibrations), respectively. These values verified the structures of the synthesized hydrazones, which were elucidated by the mass and elemental analysis. FTIR spectra of the MCH Schiff base BPH spectra is shown in Fig. 2.

^{1}H NMR Spectra

As seen in Table S3 and Fig. S2, the aromatic hydrogen peaks were observed broad range. Because the reason is that each of the two phenyl rings of the Schiff base molecule have different electron densities. So, peaks of each aromatic H atom showed distinct peaks at definite range. The hydrogen peaks of MCH generally shifted slightly to lower field compared with unsubstituted Schiff base BPH.

Table 2
Comparision of the observed and calculated vibrational spectra of the title molecule.

Mode nos.	Exp. IR (cm^{-1})	Theoretical wavenumbers (cm^{-1}) B3LYP			Characterization of normal modes with (%PED)[c]
	IR	Unscaled[a]	Scaled[b]	I_{IR}	
ν_{93}		3776	3606	30	ν_{OH} (100)
ν_{92}	3289w	3425	3271	31	ν_{NH} (99)
ν_{91}		3227	3082	0	ν_{CH} (97)
ν_{90}		3214	3069	1	ν_{CH} (98)
ν_{89}		3197	3053	1	ν_{CH} (99)
ν_{88}		3190	3047	3	ν_{CH} (99)
ν_{87}		3171	3028	6	ν_{CH} (98)
ν_{86}		3169	3026	2	ν_{CH} (97)
ν_{85}	3013vw	3155	3013	3	ν_{CH} (96)
ν_{84}		3153	3011	4	ν_{CH} (97)
ν_{83}		3102	2962	4	ν_{asCH3} (100)
ν_{82}		3070	2932	4	ν_{asCH3} (99)
ν_{81}		3035	2898	9	ν_{CH} (99)
ν_{80}	2847vw	3022	2886	11	$\nu_{s\ CH3}$ (100)
ν_{79}	1652s	1728	1671	92	$\nu_{C=O}$ (71)
ν_{78}	1602m	1661	1606	7	$\nu_{C=N}$ (44) + $\nu_{C=C}$ (29)
ν_{77}		1645	1591	21	$\nu_{C=C}$ (56)
ν_{76}		1645	1591	18	$\nu_{C=C}$ (43) + $\nu_{C=N}$ (16)
ν_{75}	1569s	1621	1568	100	$\nu_{C=C}$ (35) + δ_{CNH} (32)
ν_{74}		1600	1547	0	$\nu_{C=C}$ (62)
ν_{73}	1505s	1560	1509	40	$\nu_{C=C}$ (27) + δ_{NNH} (15)
ν_{72}		1541	1490	30	δ_{CCH} (46) + ν_{CC} (32)
ν_{71}		1495	1446	3	δ_{dCH3}(86)
ν_{70}	1439s	1490	1441	6	δ_{CCH} (43) + ν_{CC} (21)
ν_{69}		1486	1437	2	δ_{dCH3} (90)
ν_{68}		1474	1426	31	δ_{CCH} (33) + ν_{CC} (25)
ν_{67}		1439	1392	1	ν_{CC} (34) + δ_{CCH} (30)
ν_{66}		1414	1367	0	$\delta_{CH3,\ umbrella}$ (95)
ν_{65}		1393	1347	7	δ_{HCN} (29) + δ_{CCH} (18)
ν_{64}		1387	1341	35	$\nu\ _{CC}$ (36) + ν_{OC} (20) + δ_{HOC} (16) + δ_{CCO} (13)
ν_{63}	1303s	1346	1302	7	δ_{CCH} (33) + ν_{NC} (14) + $_{C=C}$ (14)
ν_{62}		1338	1294	9	δ_{CCH} (62)
ν_{61}		1334	1290	7	$_{C=C}$ (67)
ν_{60}	1253vs	1315	1272	35	$_{C=C}$ (38)
ν_{59}	1233vs	1270	1228	9	δ_{CCH} (31) + ν_{CC} (19)
ν_{58}		1251	1210	0	ν_{CC} (47) + δ_{CCH} (25)
ν_{57}		1229	1189	1	ν_{CC} (71)
ν_{56}		1202	1162	57	δ_{CCH} (33) + δ_{CCH} (26) + ν_{CC} (25)
ν_{55}	1150s	1201	1161	9	δ_{CCH} (33) + ν_{CC} (15)
ν_{54}		1179	1140	62	δ_{CCH} (45) + ν_{CC} (17) + δ_{COH} (15)
ν_{53}	1120m	1171	1132	35	δ_{CCH} (39) + ν_{NN} (18) + ν_{CC} (17)
ν_{52}		1143	1105	29	δ_{CCH} (36) + ν_{CC} (22)
ν_{51}		1128	1091	61	ν_{NN} (30) + ν_{CC} (16) + ν_{CO} (20) + δ_{CCH} (10)
ν_{50}		1075	1039	18	ν_{CO} (30) + δ_{CCC} (21) + δ_{CCH} (16)
ν_{49}		1061	1026	5	ν_{CC} (60) + δ_{CCH} (17)
ν_{48}		1060	1025	1	$\delta_{CH3\ rocking}$ (96)
ν_{47}		1034	1000	1	δ_{CCC} (34) + δ_{CCH} (31) + ν_{CC} (30)
ν_{46}		1005	972	3	$\delta_{d\ CH3}$ (91)
ν_{45}		1000	967	0	γ_{CH} (88)
ν_{44}		989	956	0	γ_{CH} (84)
ν_{43}		976	943	0	γ_{CH} (86)
ν_{42}		969	937	2	γ_{CH} (84)
ν_{41}	904vs	944	913	2	γ_{CH} (44) + γ_{NH} (33)
ν_{40}		923	893	1	ν_{CC} (27) + δ_{CNN} (16)
ν_{39}		876	847	1	γ_{CH} (83)
ν_{38}		851	822	0	ν_{CC} (44) + δ_{CCC}(16)
ν_{37}		850	822	0	γ_{CH} (94)
ν_{36}		829	802	8	γ_{CH} (74)
ν_{35}		803	776	1	γ_{CO} (58)
ν_{34}		794	767	1	ν_{CC} (68) + δ_{CCC} (17)
ν_{33}	742vs	769	744	1	ν_{CC} (39)
ν_{32}		762	737	15	γ_{CH} (71)
ν_{31}		726	702	0	γ_{CC} (50) + γ_{CH} (20)
ν_{30}		718	694	12	γ_{CC} (35) + γ_{CH} (27) + γ_{CO} (25)
ν_{29}		676	653	12	γ_{NH} (98)
ν_{28}		663	641	2	δ_{CCC} (36) + δ_{CCN} (11)
ν_{27}		650	629	9	δ_{CCO} (31) + δ_{CCC} (19)
ν_{26}		644	623	9	δ_{OCO} (23) + δ_{CCC} (22)
ν_{25}		611	590	1	δ_{CCC} (35) + δ_{CCN}(17) + γ_{CC} (15)
ν_{24}		555	537	22	γ_{OH} (87)
ν_{23}		537	519	0	δ_{CCC} (25) + δ_{CCO} (21) + γ_{CC} (13)
ν_{22}		532	515	0	τ_{CCCH} (26) + τ_{CCCC} (25) + τ_{CCCN} (15)
ν_{21}		526	508	5	τ_{CCCH} (38) + τ_{CCCC} (13)

(*continued on next page*)

Table 2 (*continued*)

Mode nos.	Exp. IR (cm^{-1})	Theoretical wavenumbers (cm^{-1}) B3LYP			Characterization of normal modes with (%PED)[c]
	IR	Unscaled[a]	Scaled[b]	I_{IR}	
ν_{20}		463	448	0	δ_{CCC} (28)
ν_{19}		428	414	3	τ_{CCCC} (40) + τ_{CCCH} (41) + τ_{CCCO} (14)
ν_{18}		419	405	0	τ_{CCCC} (60) + τ_{CCCH} (20)
ν_{17}		418	404	4	δ_{CCN} (18) + ν_{CC} (14) + δ_{CCO} (11) + δ_{CCC} (10)
ν_{16}		379	367	2	δ_{CCC}(44) + ν_{CC}(19)
ν_{15}		368	356	0	τ_{CCCC} (39) + τ_{CCNN} (22)
ν_{14}		327	316	4	δ_{CCC} (52)
ν_{13}		283	273	0	δ_{CCC} (39) + δ_{CCO} (34)
ν_{12}		263	255	1	τ_{CCNN} (19) + τ_{CCCN} (17)
ν_{11}		231	224	1	τ_{CNNC} (33) + τ_{CCCH} (18)
ν_{10}		204	197	0	δ_{CCC} (37) + δ_{CNN} (11) + ν_{CN} (11)
ν_{9}		196	189	2	τ_{CCCC} (26) + τ_{CCNN} (19)
ν_{8}		135	130	1	δ_{CCN} (34) + δ_{CCC} (33)
ν_{7}		129	125	0	τ_{CCCC} (37) + τ_{CCCN} (23)
ν_{6}		92	89	0	τ_{CCCO} (30) + τ_{CNNC} (13) + τ_{CCNN} (11)
ν_{5}		74	72	0	τ_{CCCO} (65)
ν_{4}		46	44	0	δ_{CNN} (43) + δ_{CCN} (26) + δ_{CCC} (12)
ν_{3}		43	42	0	τ_{CH3} (91)
ν_{2}		34	33	0	τ_{CCCH} (45) + τ_{CNNC} (30) + τ_{CCNN} (14)
ν_{1}		29	28	0	τ_{CCNN} (52) + τ_{CNNH} (14) + τ_{CCCH} (13)

υ, Stretching; δ, in-plane bending; γ, out-of-plane bending; τ torsion.
vs: Very strong; s: strong; m: medium; w: weak; vw: very weak.
Relative absorption intensities with highest peak absorption equal to 100.
[a] Unscaled calculated wavenumbers.
[b] Obtained from the wave numbers calculated at B3LYP/6-311++G(d,p) using scaling factors 0.967.
[c] Total energy distribution calculated B3LYP/6-311++G(d,p) level of theory. Only contributions $\geqslant$10% are listed.

The weak electron withdrawal effect of the other phenyl ring and the double bond resonance in the structure of the Schiff base caused the aromatic hydrogen peak to shift towards lower fields. Additionally, the downfield shift of the some signals indicates intramolecular and intermolecular hydrogen bonding in structure. Hydrogen bonds decrease electron density around the proton and thus shift the proton absorption to lower field.

Consequently, the aromatic hydrogen peaks were observed at δ = 6.79–8.21 ppm for MCH while in the region of δ = 6.91–7.70 ppm in BPH [26]. Theoretically, these values were found at 6.70–8.41 ppm for MCH. Also at δ = 7.69 ppm observed N—H signal in BPH, shifted δ = 8.21 ppm, and at δ = 7.53 ppm observed HC=N proton signal was observed at δ = 7.65 ppm on spectrum of MCH. N—H and HC=N proton signals in MCH were observed at δ = 11.40 ppm and δ = 7.75 ppm. Both N—H and HC=N proton signals overlapped on the aromatic H signals. Furthermore, the COOH proton signal of MCH was observed at the δ = 11.21 ppm. This value is in good agreement with literature [33]. However, this value was observed at δ = 5.57 ppm theoretically. The CH_3 groups were observed at δ = 2.33, 2.50 and one of them is attached *p*-position of 1-phenyl ring, another is present in solvent. These values were observed at δ = 2.44 and 2.52 ppm theoretically. These outcomes verified the structure of the compound MCH. The theoretically ^1H NMR spectrum of MCH is shown in Fig. S2.

The UV–Vis absorption λ_{max} values of MCH

Hydrazones absorption λ_{max} values are generally observed as two peaks at 200–350 nm region depending upon the structure. These peaks are corresponds of —N=N— and —CH=N— groups in the molecule [32–35]. The λ_{max1} peaks are sharp peaks with higher absorbance which appear at 270–350 nm corresponds to the hydrazone skeleton and the λ_{max2} peaks observed at 200–270 nm which are attributed CH=N imino groups in the molecule [32–35]. Our discussion will focus on λ_{max1} values, which are characteristic of hydrazone structure. Table S3 shows UV–Vis values of MCH and BPH hydrazones. As seen in Table S3, λ_{max1} value of MCH is 349 nm while 343 nm for BPH. Theoretically, λ_{max1} value of MCH was found 385 nm.

This can be explained: The CH_3 group is electron donating group and for that reason λ_{max1} value was expected to shift towards higher wavelength, (Bathocromic effect, shifted red). However, the inductively electron donating property of CH_3 group gradually decreased its move from the *o*-position to the *p*-position. So, the electron donating effect is diminished in CH_3 group at the *p*-position. Then, only CH_3 group cannot be responsible for the bathocromic effect. Besides, COOH is an electron withdrawing group, so it was expected that the λ_{max1} value shift towards the lower wavelength, due to the hypsochromic effect. But, the result is not in accordance with the electron withdrawing effect of COOH group. This can be explained by the formation of H-bond N—H hydrogen with oxygen of COOH group attached to the *o*-position of the phenyl ring (Fig. 3). This state augments the resonance effect, that is, it decreases its electron withdrawing ability (see Table 3).

Consequently, total effect of these substituents is an electron donating. So, λ_{max1} of compound MCH has shown a slight shift towards higher wavelength compared to BPH (bathochromic shift).

Solvent effects on the absorption λ_{max} values

Also, in this study, absorption spectra of the MCH and BPH were recorded in three different solvents with the aim of clarifying the effects of solvents. It is well-known that generally, in many dye molecules, ground state is less polar than the excited state, so that polar protic or aprotic solvents will tend to stabilize the excited state more than the ground state. As seen in Table S4, hydrazone dye should be more stabile case excited state than the ground state in methanol and ethanol according to acetone solutions. Therefore, λ_{max} values have shown a slight shift towards bathochromic region in methanol and ethanol solutions according to acetone solution.

Description of the crystal structure of N-(4-Methylbenzylidene)-N′-(2-carboxyphenyl hydrazine

The structure of N-(4-Methylbenzylidene)-N′-(2-carboxyphenyl hydrazone, crystallizes into a monoclinic lattice with space group $P2_1/c$. An ORTEP view of the asymmetric unit is shown in Fig. 1

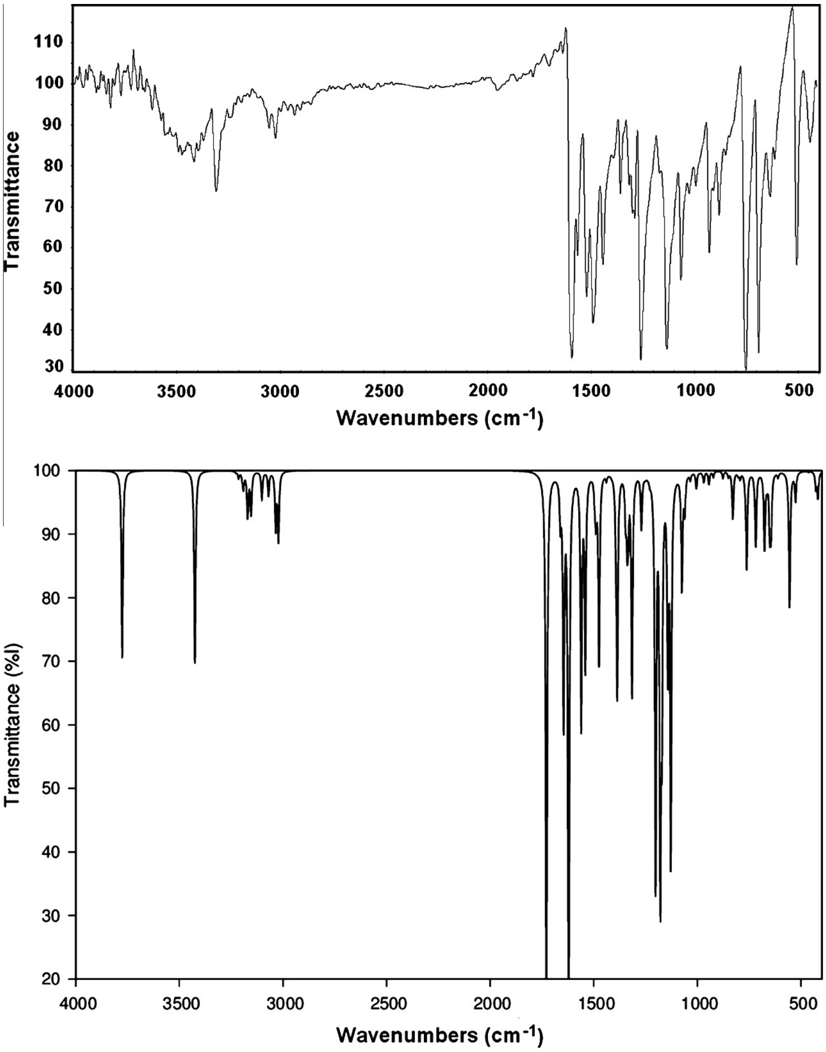

Fig. 2. FTIR spectra of the (a) MCH Schiff base and (b) BPH spectra.

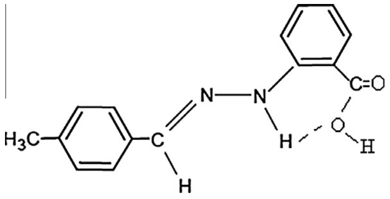

Fig. 3. The formation hydrogen bond between the COOH and N—H groups.

and bond distances and angles are presented in Table S1. The asymmetric unit contains one molecule. The molecule adopts an (E)-configuration about the azomethine C_8—N_2 double bond with, an N_1—N_2—C_8—C_5 torsion angle of −178.1(3). The dihedral angle between the planes of the methylphenyl and carboxyphenyl ring is 7.2(2)°. Hence, the molecule is almost planar The N_1—C_9, N_1—N_2 bonds distances are between 1.381(4) and 1.367(4) Å, respectively. The N2—C8 double bond is 1.271(4) Å. All the bond distances in the molecule are within normal ranges comparable to those of the similar compounds [1,26,36,37]. The bond distances, bond angles and hydrogen bonding are comparable with the literature [1,26,36–39]. Except for H8 and H1N, the H atoms were positioned geometrically, with C—H = 0.93 Å and O—H = 0.82 Å, and constrained to ride on their parent atoms, with $U_{iso}(H) = 1.2U_{eq}(C,O)$. Also, the methyl H atoms were positioned geometrically, with C—H = 0.96 Å and $U_{iso}(H) = 1.5U_{eq}(C)$. As shown in Fig. 4, each enantiomer forms head-to-tail molecular pairs. Also, an interesting feature of this structure is the presence of one intramolecular and one intermolecular N—H···O and O—H···O hydrogen bonds which stabilize this conformation, respectively, [N(1)—H(1N)···O(1)] and [O(2)—H(2)···O(1)] in carboxyl group of molecule. Intra-intermolecular hydrogen bond distances and bond angles are listed in Table 4. Also, dimeric structure can be seen from the packing diagram (Fig. S3). Intermolecular π–π and hydrogen bonding interactions link the molecules and these interactions play an important role in the stabilization of the crystal structure. If a comparison to be made with BPH molecule, the bond distances corresponding N_1—C_9, N_1—N_2 bonds and N_2—C_8 double bond are 1.435(10), 1.330(8) and 1.312(9) Å, respectively [40]. While the C_9—N_1—N_2, N_1—N_2—C_8, and N_2—C_8—C_5 bond angles in MCH molecule are 120.2(3)°, 116.8(3)° and 121.7(3)°, bond angles corresponding to them in BPH are 119.3(6)°, 117.5(5)° and 120.9(6)° respectively. Also, there is no intermolecular hydrogen bonding in BPH molecule [31]. Moreover, the theoretical values of bond distances, bond angels and torsion angles of MCH can be seen in Table S1. As seen from Table S1, the results of X-ray diffraction analyses are consistent with the theoretical values.

Table 3
UV–Vis absorption λ_{max} values of the hydrazones in various solvents.

Abbrev.	Methanol (10^{-5}M)		Ethanol (10^{-5} M)		Acetone (10^{-5} M)		B3LYP 6-31G++(d, p)(in Methanol)	
	λ_{max1} (nm) (Abs.)	λ_{max2} (nm) (Abs.)	λ_{max1} (nm) (Abs.)	λ_{max2} (nm) (Abs.)	λ_{max1} (nm) (Abs.)	λ_{max2} (nm) (Abs.)	λ_{max1} (nm) (Abs.)	λ_{max2} (nm) (Abs.)
BPH	343 (0.965)	250 (0.851)	344 (0.948)	236 (0.558)	342 (0.971)	325 (0.724)		
MCH	349 (1.485)	268 (0.275)	350 (3.000)	225 (2.646)	347 (1.258)	337 (1.317)	385	345

Note: Between the screen 900–200 nm.

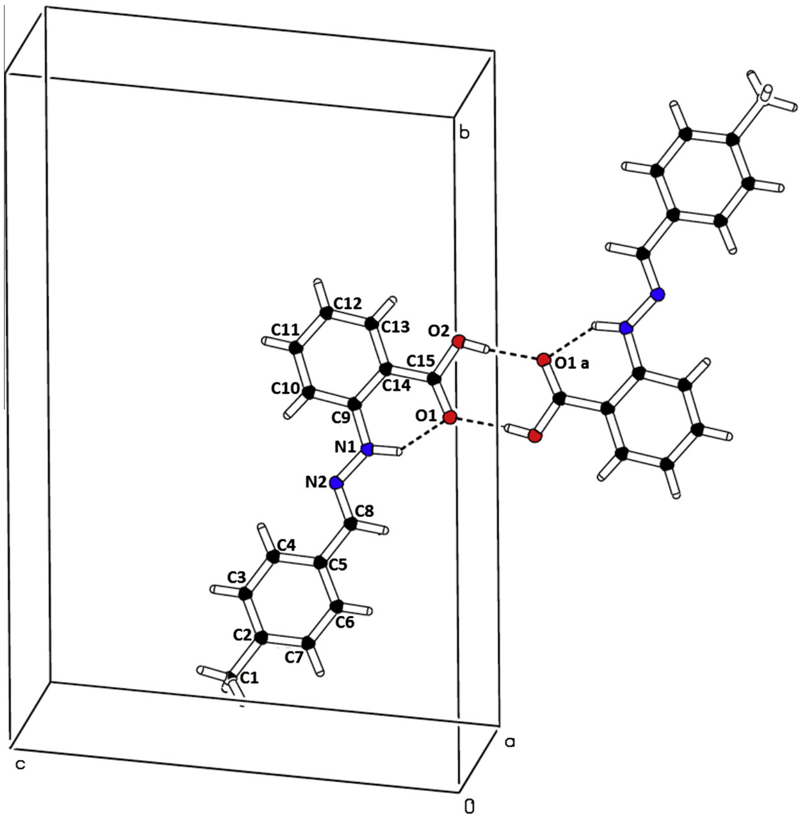

Fig. 4. The molecular structure of compound, showing the intra-and intermolecular hydrogen bonding. Intra-intermolecular O—H···N and O—H···O hydrogen bonds are shown as dashed.

Table 4
The hydrogen bond distances (Å) and angle (°).

D—H···A	d(D—H) (Å)	d(H···A) (Å)	d(D···A) (Å)	D—H···A (°)
N1—H1N—O1	0.91	1.89	2.668(5)	143
O2—H2—O1^{i}	0.82	1.81	2.626(5)	173

Symmetry code: (i) = 4 − *x*, −*y*, 1 − *z*.

An interesting comparison can be made with the structure of N-Benzlidene-N′-(2-carboxyphenyl) hydrazine (BCH) [37] which do not contain a methyl group different from MCH molecule. The structure of BCH crystallizes into monoclinic lattice with space group $P2_1/n$. The molecule of BCH takes up E conformation and the dihedral angle between the planes of the phenyl and carboxyphenyl rings is 4.9(1)° [37]. In BCH molecule, the bond distances corresponding $N_1—C_9$, $N_1—N_2$ bonds and $N_2—C_8$ double bond are 1.364(4), 1.360(3) and 1.268(4) Å respectively. Also, in BCH molecule, the bond angles corresponding $C_9—N_1—N_2$, $N_1—N_2—C_8$ and $N_2—C_8—C_5$ are 115.5(3), 120.1(3) and 122.1(3), respectively [37]. Moreover, while the $O_1—C_{15}—O_2$ bond angle in BCH molecule is 120.3(3)°, bond angle corresponding to it in MCH is 121.8(3)°.

Conclusions

In this study, MCH was synthesized by the condensation reaction of 2-hydrazinobenzoic acid and 4-metylbenzaldehyde. The spectral data and crystal structure of MCH molecule were compared with BPH molecule. Also, the spectral data and crystal structure of MCH were compared with theoretical results. Analysis of spectral data show that total effect both as the electron donating group, CH_3, and a H-bond made *o*-COOH group behave as an electron donating group. So, λ_{max1} of compound MCH has shown a slight shift towards higher wavelength compared to BPH bathochromic shift, namely red shift. Furthermore, solvent effect on the UV–Vis. absorption behavior was investigated and it was observed that the more solvent polarity increases, the more shifting happens to the absorption λ_{max} value to the bathochromic region. On the other hand, all the bond distances and bond angles are within normal ranges and comparable with those of similar compounds. The crystal structure is stabilized by the intermolecular O—H···O and intramolecular N—H···O hydrogen bonding interaction. This result is confirmed via both spectral and X-ray values.

Appendix A. Supplementary material

Supplementary data associated with this article can be found, in the online version, at http://dx.doi.org/10.1016/j.saa.2014.02.104.

References

[1] T. Tunc, H. Tezcan, M. Sari, O. Büyükgüngör, R. Yagbasan, Acta Cryst. C 59 (2003) 528.
[2] H.K. Fun, K.V. Sujith, P.S. Patil, B. Kalluraya, S. Chantrapromma, Acta Cryst. E 64 (2008) 1961.
[3] K.K. Bedia, O. Elcin, U. Seda, K. Fatma, S. Nathaly, R. Selvim, A. Dimoglo, Eur. J. Med. Chem. 41 (2006) 1253.
[4] S.G. Kucukguzel, S. Rollas, I. Kucukguzel, M. Kiraz, Eur. J. Med. Chem. 34 (1999) 1093.
[5] R. Maccari, R. Ottana, M.G. Vigorita, Bioorg. Med. Chem. Lett. 15 (2005) 2509.
[6] V. Raparti, T. Chitre, K. Bothara, V. Kumar, S. Dangre, C. Khachane, S. Gore, B. Deshmane, Eur. J. Med. Chem. 44 (2009) 3954.
[7] J. Easmon, G. Pürstinger, K.S. Thies, G. Heinisch, J. Hofmann, J. Med. Chem. 49 (2006) 6343.
[8] V. Onnis, M.T. Cocco, R. Fadda, C. Congiu, Bioorg. Med. Chem. 17 (2009) 6158.
[9] M.C.R. Argüelles, R. Cao, A.M. García-Deibe, C. Pelizzi, J.S. Matalobos, F. Zani, Polyhedron 28 (2009) 2187.
[10] V Getautis, M. Daskeviciene, T. Malinauskas, V. Gaidelis, V. Jankauskas, Z. Tokarski, Synth. Met. 155 (2005) 599.
[11] P. Hohenberg, W. Kohn, Phys. Rev. 136 (1964) 136.
[12] W. Kohn, L. Sham, Phys. Rev. 140 (1965) A1133.
[13] M.J. Frisch, G.W. Trucks, H.B. Schlegel, G.E. Scuseria, M.A. Robb, J.R. Cheeseman, G. Scalmani, V. Barone, B. Mennucci, G.A. Petersson, H. Nakatsuji, M. Caricato, X. Li, H.P. Hratchian, A.F. Izmaylov, J. Bloino, G. Zheng, J.L. Sonnenberg, M. Hada, M. Ehara, K. Toyota, R. Fukuda, J. Hasegawa, M. Ishida, T. Nakajima, Y. Honda, O. Kitao, H. Nakai, T. Vreven, J.A. Montgomery, Jr., J.E. Peralta, F. Ogliaro, M. Bearpark, J.J. Heyd, E. Brothers, K.N. Kudin, V.N. Staroverov, T. Keith, R. Kobayashi, J. Normand, K. Raghavachari, A. Rendell, J.C. Burant, S.S. Iyengar, J. Tomasi, M. Cossi, N. Rega, J.M. Millam, M. Klene, J.E. Knox, J.B. Cross, V. Bakken, C. Adamo, J. Jaramillo, R. Gomperts, R.E. Stratmann, O. Yazyev, A.J. Austin, R. Cammi, C. Pomelli, J.W. Ochterski, R.L. Martin, K. Morokuma, V.G. Zakrzewski, G.A. Voth, P. Salvador, J.J. Dannenberg, S. Dapprich, A.D. Daniels, O. Farkas, J.B. Foresman, J.V. Ortiz, J. Cioslowski, D.J. Fox, Gaussian 09, Revision B.01, Gaussian Inc., Wallingford CT, 2010.
[14] T. Vladimiroff, J. Mol. Struct. Theochem. 453 (1998) 119.
[15] C.T. Lee, W.T. Yang, R.G. Parr, Phys. Rev. B 37 (1988) 785.
[16] R.G. Parr, W. Yang, Density Functional Theory of Atoms and Molecules, Oxford University Press, New York, 1989.
[17] A.D. Becke, J. Chem. Phys. 98 (1993) 5648.
[18] P.J. Stephens, F.J. Devlin, C.F. Chabalowski, M.J. Frisch, J. Phys. Chem. 98 (1994) 11623.
[19] P. Pulay, G. Fogarasi, G. Pongor, J.E. Boggs, A. Vargha, J. Am. Chem. Soc. 105 (1983) 7037.
[20] G. Rauhut, P. Pulay, J. Phys. Chem. 99 (1995) 3093.
[21] J.E. McMurry, Organic Chemistry, Brooks/Cole, CA, 2004.
[22] Rigaku Americas and Rigaku CRYSTAL-CLEAR Program for Integration of the Intensities, Correction for Lorentz and Polarization Effects and Cell Refinement, Rigaku Americas, The Woodlands, Texas, and Rigaku Corporation, Tokyo, 2005.
[23] G.M. Sheldrick, Acta Cryst. A 46 (1990) 467.
[24] G.M. Sheldrick, SHELXL97 Program for Crystal Structure Refinement, University of Göttingen, 1997.
[25] L.J. Farrugia, J. Appl. Cryst. 30 (1997) 565.
[26] T. Tunc, H. Tezcan, E. Sahin, N. Dilek, Mol. Cryst. Liq. Cryst. 552 (2011) 194.
[27] P. Gilli, V. Bertolasi, L. Pretto, G. Gilli, J. Mol. Struct. 790 (2006) 40.
[28] L.J. Bellamy, The Infrared Spectra of Complex Molecules Methuen, London, 1962.
[29] N.B. Colthup, L.H. Daly, S.E. Wiberley, Introduction to Infrared and Raman Spectroscopy, Academic Press, New York, 1990.
[30] B.C. Smith, Infrared Spectral Interpretation: A Systematic Approach, CRC Press, Washington DC, 1999.
[31] H. Tezcan, N. Ozkan, Dyes Pigments 56 (2003) 159.
[32] H. Tezcan, E. Uzluk, Dyes Pigments 76 (2008) 733.
[33] H. Tezcan, E. Uzluk, Dyes Pigments 75 (2007) 633.
[34] N. Karabocek, A. Kucukdumlu, P. Ekmekcioglu, S. Karabocek, J. Macromol. Sci. Pure 46 (2009) 1007.
[35] L.V. Ababei, A. Kriza, A.M. Musuc, C. Andronescu, E.A. Rogozea, J. Therm. Anal. Calorim. 101 (2010) 987.
[36] T. Tunc, M. Sari, R. Yagbasan, H. Tezcan, E. Sahin, Acta Cryst. C 59 (2003) 192.
[37] H. Tezcan, T. Tunc, E. Sahin, R. Yagbasan, Anal. Sci. 20 (2004) 137.
[38] S. Shanmuga, S. Raj, H.K. Fun, Z.L. Lu, W. Xiao, X.Y. Gong, B.Z. Kang, Acta Cryst. C 55 (1999) 942.
[39] S. Shanmuga, S. Raj, H.K. Fun, Z.L. Lu, W. Xiao, X.Y. Gong, C.M. Gen, Acta Cryst. C 56 (2000) 1013.
[40] B.B. Vickery, G.R. Willey, Acta Cryst. C 41 (1985) 1072.